2778 *Biochemistry* **2010,** *49,* 2778–2785
DOI: 10.1021/bi902003g

BIOCHEMISTRY
including biophysical chemistry & molecular biology
Article

A Temperature-Induced Narrow DNA Curvature Range Sustains the Maximum Activity of a Bacterial Promoter in Vitro[†]

Gianni Prosseda,[‡] Alessia Mazzola,[‡,∥] Maria Letizia Di Martino,[‡] Denis Tielker,[‡,⊥] Gioacchino Micheli,[§] and Bianca Colonna*[,‡]

[‡]*Istituto Pasteur Fondazione Cenci Bolognetti, Dip. Biologia Cellulare e dello Sviluppo, Sapienza Univ. Roma, via dei Sardi 70, 00185 Roma, Italy, and* [§]*Istituto di Biologia e Patologia Molecolari IBPM CNR, c/o Sapienza Univ. Roma, Dip. Genetica e Biologia Molecolare, P.le A. Moro 5, 00185 Roma, Italy.* [∥]*Present address: Istituto Superiore di Sanità, Dip. Biologia Cellulare e Neuroscienze, V. le Regina Elena 299, 00161 Roma, Italy.* [⊥]*Present address: Institut für Mikrobiologie, Molekulare Mykologie, Heinrich-Heine-Universität, Universitätsstrasse 1, 40225 Düsseldorf, Germany.*

Received November 21, 2009; Revised Manuscript Received February 10, 2010

ABSTRACT: Among the molecular strategies bacteria have set up to quickly match their transcriptional program to new environments, changes in sequence-mediated DNA curvature play a crucial role. Bacterial promoters, especially those of mesophilic bacteria, are in general preceded by a curved region. The marked thermosensitivity of curved DNA stretches allows bacteria to rapidly sense outer temperature variations and affects transcription by favoring the binding of activators or repressors. Curved DNA is also able to influence the transcriptional activity of a bacterial promoter directly, without the involvement of trans-acting regulators. This study attempts to quantitatively analyze the role of DNA curvature in thermoregulated gene expression using a real-time in vitro transcription model system based on a specific fluorescence molecular beacon. By analyzing the temperature-dependent expression of a reporter gene in a construct carrying a progressively decreasing bent sequence upstream from the promoter, we show that with a decrease in temperature a narrow curvature range accounts for a significant enhancement of promoter activity. This strengthens the view that DNA curvature-mediated regulation of gene expression is likely a strategy offering fine-tuning control possibilities and that, considering the widespread presence of curved sequences upstream from bacterial promoters, it may represent one of the most primitive forms of gene regulation.

The view that architectural features of a genome might hold functional relevance is gaining wide acceptance. On a local scale, intrinsic structural properties of DNA, while ultimately relying on the primary sequence of the molecule, may constitute spatial features available as additional coregulatory resources for essential cell processes. Sequence-directed DNA curvature, often also indicated as intrinsic bending, is a widespread example of such a resource. It was initially identified as originating from the helically phased distribution of short A-tracts along kinetoplast DNA of trypanosome species, and while the functional significance of such DNA regions in those organisms is as yet unclear (*1*), a wealth of experimental evidence has built up, revealing the existence of intrinsically curved DNA in a broad spectrum of biological systems, elucidating its chemical and physical properties and stressing its regulatory potential as a local architectural feature of the genome (*2*−*5*).

Within the broad collection of processes affected or strongly surmised of being influenced by sequence-directed DNA curvature (*5*−*7*), transcriptional regulation ranks among those with a major impact on cell life and adaptability to changing environmental conditions (*8*−*10*). In this respect, bacterial genomes constitute a paradigmatic case. Genome-wide studies have revealed conservative distribution patterns of intrinsically curved DNA in mesophilic bacteria: a substantial proportion of the promoters is characterized by intrinsic bends, located either within the promoters themselves or 100−200 bp upstream from the nearest transcription start (*11*−*13*). Upstream curved sequences (UCS)[1] are widely distributed also in archeal genomes with the exception of hyperthermophilic prokaryotes, thus suggesting that UCS are evolutionarily preserved and likely determined by temperature-mediated selection in connection with the cell habitat (*14*, *15*). The analysis of regulatory regions from a large collection of bacterial and archeal genomes has revealed that bent DNA could be even considered a conserved regulatory element in some families of orthologous genes, spanning a broad spectrum of biological functions and including genes encoding nucleoid proteins like HU, IHF, and FIS (*16*).

In bacteria, transcriptional regulation by bent DNA has been demonstrated in a large number of cases (*10*, *17*−*22*). On the one hand, static DNA curvature has been shown to activate transcription by facilitating the binding of RNA polymerase (RNAP) to promoters or by favoring the interaction of activators. This is

[†]This work was supported by grants from Ministero Istruzione Università e Ricerca (MIUR 2008) and Sapienza Università di Roma (Ateneo/Facoltà 2007, 2008) to B.C. and G.P. and from Consiglio Nazionale delle Ricerche (IBPM 2007, 2008) to G.M. D.T. was a recipient of a fellowship within the postdoctoral program of the German Academic Exchange Service (DAAD).

*To whom correspondence should be addressed. E-mail: bianca.colonna@uniroma1.it. Telephone: +39 0649917582. Fax: +39 0649917594.

[1]Abbreviations: cat, chloramphenicol acetyltransferase; DACBCYL, 4-[4′-(dimethylamino)phenylazo]benzoic acid; dPTP, 6-(2-deoxy-β-D-ribofuranosyl)-3,4-dihydro-8*H*-pyrimido[4,5-*c*][1,2]oxzin-7-one triphosphate; FAM, 5-iodoacetamidofluorescein; MB, molecular beacon; RNAP, RNA polymerase; UCS, upstream curved sequences.

 Published on Web 02/19/2010

exemplified by the nucleoid proteins IHF, FIS, and HU, which are known to recognize curved DNA and may themselves enhance DNA bending (*10*, *23*−*28*). On the other hand, curved DNA regions can also repress transcription initiation. In this case, DNA curvature generally plays an indirect role: the binding of specific silencers stabilizes or enhances a preexisting DNA loop, thus effectively blocking transcription of downstream regions (*17*, *19*−*21*). Among these silencers, H-NS has been extensively studied, since in enterobacteria it affects the expression of a large number of unrelated genes encoding housekeeping functions as well as virulence factors. The molecular basis of its regulatory activity probably resides in its preferential interaction with intrinsically curved DNA and in its ability to induce bending of noncurved DNA, possibly also altering DNA topology (*29*, *30*). As far as *Escherichia coli* is concerned, the relevance of bent DNA to gene regulation has been stressed by recent in silico studies revealing that almost all global regulators, including the nucleoid proteins mentioned above, have a marked tendency to control operons carrying UCS (*22*). The same studies also show that many genes encoding global as well as specific regulators contain UCS themselves, suggesting that curvature changes in these promoters could indirectly affect the expression of the genes controlled by these regulators.

In previous studies, we have demonstrated a new role for curved DNA, which expands the functional significance of bent regions beyond the one of mere steric flag for regulatory factors: a curved DNA tract can behave as a thermosensor that optimizes gene regulation in response to outer temperature changes by gradually unmasking specific target sites for cofactors involved in transcription activation or repression (*17*, *19*, *26*). In particular, this feature accounts for the strict temperature dependence of the virulence phenotype in *Shigella*, a pathogenic microorganism that is able to invade the intestinal epithelium in humans. Upon entry of the bacterium into the host cell, the activation of *virF*, a gene encoding the first positive activator of the virulence cascade, occurs only at permissive temperatures, i.e., >32 °C (*19*). At nonpermissive temperatures, H-NS represses *virF* expression by interacting with two sites encompassing a bent region within the *virF* promoter. The accessibility of the target DNA to H-NS varies significantly as a function of temperature both in vitro and in vivo and is related to a sudden curvature alteration occurring at the transition temperature (*17*).

A strict correlation between DNA curvature and thermoregulated expression has also been reported in other microorganisms. A model closely resembling the one proposed for the *Shigella virF* system has been postulated for the *Yersinia virF* gene and also for the *E. coli hly* operon. In *Yersinia*, a stronger curvature of the *virF* promoter allows the stable binding of the YmoA repressor, thereby causing the silencing of the virulence genes on the Yop plasmid (*20*). In the *E. coli hly* operon, the promoter contains two H-NS binding sites separated by a large DNA tract endowed with a bent structure. At low temperatures, a stronger curvature of this region favors the formation of a H-NS−promoter nucleocomplex, which occludes the access to RNAP (*21*). While in the mentioned cases the increase in DNA curvature induced by low temperatures affects gene expression negatively, the opposite effect has been observed in other systems. Indeed, in *Clostridium perfringens*, the increased curvature of the *plc* promoter arising at low temperatures triggers the expression of the corresponding gene, even without involving additional trans-acting regulators (*18*). A further example is represented by the λ bacteriophage P_L promoter, in which the increased curvature at low temperatures favors the transcriptional activity through the formation of a ternary complex involving template DNA, RNAP, and the IHF protein (*23*).

The collection of available experimental data raises the issue of whether an optimal curvature level that is able to influence gene expression exists. The evidence that intrinsic curvature of prokaryotic promoters significantly affects gene regulation is convincing; nevertheless, it is worth remembering that often different curvature levels have been obtained by using fragments differing in length and/or in base composition and that, as far as the involvement of DNA curvature in thermoregulated gene expression is concerned, systematic studies covering a wide range of temperatures are lacking. This study is an attempt to quantitatively analyze the role of DNA curvature in thermoregulated gene expression using an in vitro transcription model system. By analyzing the temperature-dependent expression of a reporter gene in a construct carrying a progressively decreasing bent sequence such as UCS, we show that with a decrease in temperature a narrow curvature range accounts for a significant enhancement of promoter activity.

EXPERIMENTAL PROCEDURES

Bacterial Strains and General Procedures. *E. coli* K12 DH10b (F′Δ[*mrr hsd*rms *mcr*BC] φ80dlacZΔM15 Δ*lac*X74 *deoR recA*1 *araD*139 Δ[*araleu*]7697 *galU galK rpsL endA1 nupG*) (*31*) was used as a recipient of recombinant plasmids. When required, the following antibiotics and chemicals were added to the culture medium: 50 μg/mL ampicillin, 75 μg/mL chloramphenicol, and 50 μg/mL streptomycin. Isolation of plasmids, restriction digestions, cloning, polymerase chain reactions (PCRs), electrophoresis, and purification of DNA fragments were conducted as described previously (*17*). The sequence of the PCR-generated fragments was checked by the dideoxy chain terminating method (*31*).

Plasmid Constructs. Plasmid pPK201/CAT (*32*) is a pSP65 derivative containing a highly bent 211 bp fragment from kinetoplast DNA of *Crithidia fasciculata*. The pCf plasmid series was obtained by cloning the curved inserts generated by in vitro mutagenesis (see below) of pPK201/CAT into the BamHI site of pUC18. pCAT is a vector we have constructed to analyze the transcriptional contribution of promoter upstream regions: it has been obtained by cloning a reporter chloramphenicol resistance gene, including its promoter boxes (−35 and −10) and an upstream BglII restriction site, into a pBR322 derivative (Figure 3A). The pCATCf plasmids have been generated by cloning pCf inserts into the BglII site of pCAT: the inserts were obtained upon PCR amplification of the pCf plasmids with the LK1 (5′-CTCGGTACCCGGAGATCT-3′) and LK2 (5′-AGGTCGACTCTAGAGGATCC-3′) oligo pair, modified to contain a BamHI and BglII site, respectively. All pCATCf plamids used in this study were checked by sequencing to carry the insert in the same orientation (NruI site in the distal position as compared to the −35 box).

In Vitro Mutagenesis. Mutagenesis experiments were performed according essentially to the protocol proposed by Zaccolo et al. (*33*), using the nucleotide analogue dPTP [6-(2-deoxy-β-D-ribofuranosyl)-3,4-dihydro-8*H*-pyrimido[4,5-*c*][1,2]oxzin-7-one triphosphate (Amersham Life Sciences)]. Plasmid pPK201/CAT was amplified as follows, using *Taq* polymerase and the forward and reverse primers CriF (5′-TATGACCATGATTACGCCAAG-3′) and CriR (5′-ATAGAATACACGGAATTCGAGC-3′), respectively, both located outside the BamHI site. The 20 μL

PCR mixtures in buffer R [2 mM $MgCl_2$, 10 mM Tris-HCl (pH 8.3), 50 mM KCl, and dATP, dCTP, dGTP, and dTTP at 200 mM each] contained increasing concentrations of dPTP (30, 60, 90, and 120 nM each). After 30 cycles (1 min at 95 °C, 1 min at 56 °C, and 1 min at 72 °C), 1 μL from each reaction mixture was diluted to 100 μL with buffer R (dPTP was not further added) and used as template in a second round of PCR (25 cycles of 1 min at 95 °C, 1 min at 45 °C, and 1 min at 72 °C), primed by the same primer pair. The reaction products were then restricted with BamHI and ligated to the BamHI-linearized pUC18 vector. The ligation products were used to transform DH10b cells. Eight Ap^r clones from each PCR were checked for the presence of a Cf insertion using PCR analysis with oligos LK1 and LK2 (see Plasmid Constructs). A total of 19 recombinant pCf plasmids were then sequenced and used in in vitro electrophoretic mobility assays. The control plasmid (pCf0) was obtained following the same approach, conducted in the absence of dPTP during the PCR steps. Sequencing proved the insert of this plasmid to be identical to that of pPK201/CAT.

DNA Curvature Assays. pCf plasmids were amplified with the LK1 and LK2 oligo pair (see Plasmid Constructs), and the resulting amplicons were digested with BamHI and BglII, generating 219 bp fragments. The pCATCf plasmids were amplified by PCR using the forward primer CatF (5′-AAGTTGGAACC-TCTTACGTGC-3′) and the reverse primer CatR (5′-TGCG-TCCGGCGTAGAGGATCG-3′), located in the vector and in the *cat* coding region, respectively, generating 271 bp fragments. The electrophoretic mobility of the pCf and pCATCf inserts was compared to that of unbent marker fragments (Pharmacia's 100 bp ladder) by electrophoresis on 0.75 mm thick 5% polyacrylamide gels [29.2:0.8 acryl:bis in 90 mM Tris-HCl, 90 mM H_3BO_3, and 2.5 mM Na_2EDTA (pH 8.6)] run at 5 V/cm with constant buffer recirculation. Gels were run at 4 °C and, in the case of pCATCf inserts, also at the same temperatures used in the in vitro transcription assays, using a water-jacketed apparatus as previously described (*19*). The gel temperature, monitored by means of a thin probe, remained constant within ±0.3 °C throughout the run.

In Vitro Transcription. Transcriptional activity was assayed in vitro by a real-time monitoring approach based on the use of a template-specific antisense fluorescent molecular beacon (*34*). The *cat* gene-specific beacon probe used in this study (*cat*-MB) is shown in Figure 3B. It was designed on the basis of a computer-predicted *cat* mRNA secondary structure, to identify a suitable single-stranded region. The stem of the beacon carries a fluorophore [5-iodoacetamidofluorescein (FAM)] at the 5′-end and a quencher {4-[4′-(dimethylamino)phenylazo]benzoic acid (DABCYL)} at the 3′-end. In the absence of a target transcript, nucleotide pairing in the stem keeps the quencher close enough to the fluorophore, resulting in very low fluorescence. With ongoing transcription, the presence of a specific template allows the looped sequence of the beacon to stably interact with its target, separating the fluorophore from the quencher to an extent sufficient to give rise to measurable fluorescence (T_m of *cat*-MB = 60 °C). In vitro transcription reactions (50 μL) were set up in 96-well plates in a pH 7.9 Tris-buffered mix containing 500 nM dNTP, 5 mM $MgCl_2$, 100 μg/mL BSA, 4 μg/mL pCAT-Cf plasmid DNA, 10^{-4} mM *cat*-MB, and 20 units/mL RNAP [RNA polymerase (Epicenter)]. The reaction progress was monitored with a Victor 1420 (Wallac) fluorimeter at different temperatures (27.1, 28.5, 30.9, 33.6, 36, and 37.4 °C), using an excitation wavelength of 485 nm and an emission wavelength of 530 nm. Final readings were taken after reaction for 30 min. As a background control we used reactions run under the same conditions in the absence of RNAP. We validated the *cat*-MB probe by running the mixtures from individual pCATCf reactions and from control reactions [set up, at all temperatures considered, either with an unspecific template (pBR322), in the absence of RNAP, or in the absence of the *cat*-MB probe] on agarose gels and by analyzing fluorescence emission in a Typhoon 9200 scanner (Amersham). A specific "anti-beacon" DNA (a-*cat*-MB; coordinates 448−467 of the *cat* sequence) was used to obtain a further specificity control.

Software. Computer-generated predictions of DNA curvature were obtained with DICE (DNA Intrinsic Curvature Evaluator), a program developed by one of the authors (G.M.) for the analysis of intrinsic bending. The program is basically an implementation of the CURVATURE algorithm (*35*) on DOS/Windows platforms and can use different sets of dinucleotide roll, tilt, twist, and rise estimates to generate wedge and direction angles. RNA structure predictions for constructing the molecular beacon were obtained with RNAdraw version 1.1.b2 (*36*). Statistical evaluations, plotting, and curve fitting were conducted with the aid of commercial software (OriginPro, Prism, and Excel).

RESULTS AND DISCUSSION

Generation of Fragments with Progressively Decreasing Curvature. The DNA curvature of the 211 bp fragment from kinetoplast DNA of *C. fasciculata* is a very well-known example of intrinsic bending strictly depending on the occurrence of helically phased A-stretches (*2*, *4*, *32*, *37*). To generate a series of equally sized fragments with progressively decreasing curvature, we attempted to mutagenize the A-rich oligonucleotide regions of the 211 bp *C. fasciculata* fragment. This was done by a random mutagenesis protocol we successfully used previously on the promoter of the *Shigella virF* gene (*17*). The approach relies on the efficient incorporation of the nucleotide analogue dPTP during in vitro DNA amplification, determining mainly A → G and T → C transitions (*33*). Briefly, upon amplification of the pPK201/CAT region containing the 211 bp *C. fasciculata* bent fragment in the presence of increasing concentrations of dPTP (0, 30, 60, 90, and 120 nm), the mutations were fixed by a second amplification round without further addition of dPTP.

The resulting amplicons were digested and cloned into the BamHI site of pUC18, generating the pCf plasmid series. Eight Ap^r-resistant transformants were randomly selected from each mutagen concentration. Their plasmids, as well as a control one (pCf0, obtained by the same procedure but in the absence of dPTP), were screened for the presence of an insert. Inserts of the expected size (223 nucleotides) were further analyzed for intrinsic bending by polyacrylamide gel electrophoresis under temperature conditions (4 °C) that maximized the effect of DNA curvature on electrophoretic mobility (*2*, *4*, *38*). The PAGE pattern (Figure 1) indicates that the mutagenesis protocol we have used is able to generate a spectrum of equally sized fragments covering a wide range of curvature values (*k* factor, i.e., ratio between apparent size and real size, ranging from 2.91 to 1.07; wild-type value of 3.82), which clearly tend to decrease with an increase in dPTP concentration. In particular, the very low *k* value (1.07) of insert pCf19 strongly suggests that the DNA curvature of this fragment has been thoroughly disrupted.

The inserts of 10 recombinant plasmids (pCf2, pCf4, pCf5, pCf 7, pCf8, pCf10, pCf11, pCf13, pCf14, and pCf19), selected at random and covering the entire curvature range generated by the

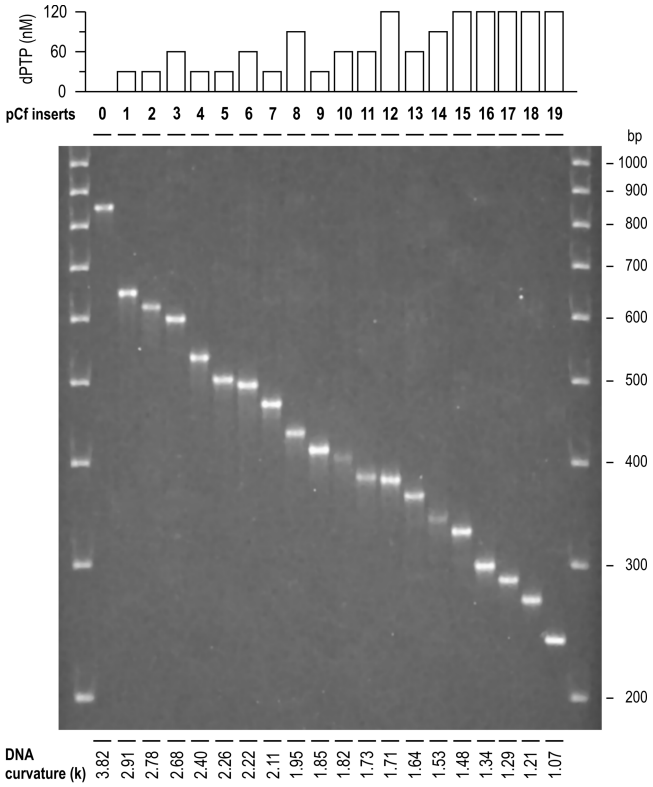

FIGURE 1: Mutagenesis of the bent fragment from kinetoplast DNA of *C. fasciculata*. DNA fragments (223 nucleotides), containing the 211 bp curved sequence of *C. fasciculata* kinetoplast DNA (Cf0) or its derivatives obtained upon random mutagenesis with different concentrations of PTP (indicated in the histogram at the top), were run at 4 °C on a polyacrylamide gel. An unbent 100 bp DNA fragment ladder was used as a size marker. Gel staining was conducted with ethidium bromide. DNA curvature (*k*, ratio of the apparent size to the real size) is shown below each lane. Each value is the average of at least three independent gel runs; the difference between the minimum and maximum observed values did not exceed 2.1% of the average.

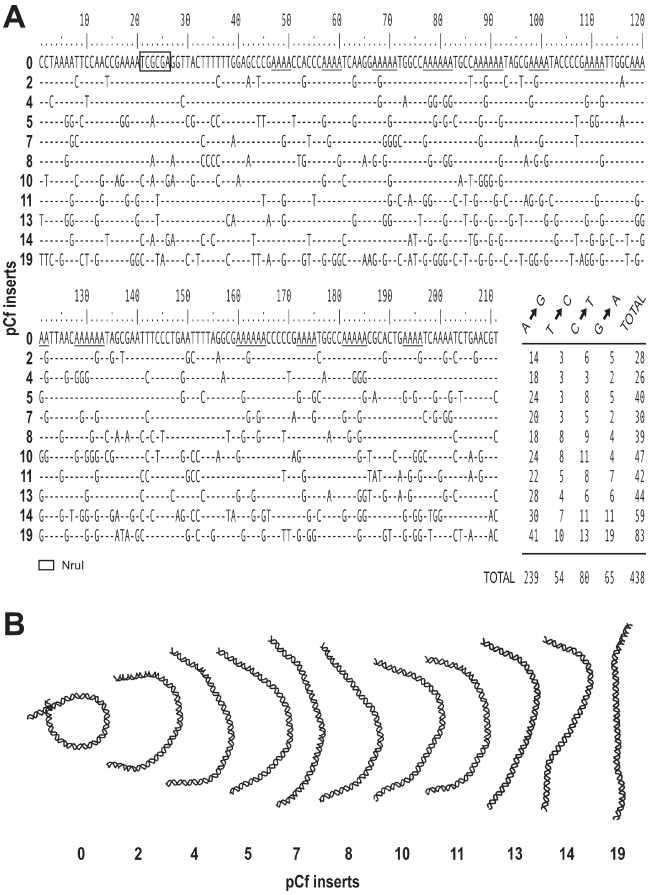

FIGURE 2: Mutagenized pCf inserts. Sequences and curvature predictions. (A) Nucleotide sequence of a subset of the pCf inserts obtained after in vitro mutagenesis and analyzed for the presence of curvature in Figure 1 (only the 211-nucleotide core region is shown). Cf0 represents the wild-type insert. Helically phased A-rich tracts, known to give rise to the curved structure, are underlined. The number and type of mutations are summarized in the table to the right of the sequences. (B) Computer predictions of the sequences shown in panel A. Models are presented in decreasing DNA curvature order. Nucleotide position 1 of panel A corresponds to the left end (pCf0 model) or to the top end (remaining models).

mutagenesis protocol, were compared by sequencing with the insert from control plasmid pCf0 (Figure 2A). Mutational events appear to have occurred over the entire span of the 211 bp bent region, and the number of mutations per helix turn (m/ht) tends to increase with an increase in dPTP concentration (Figure 1). Mutations were mainly determined by A → G transitions (Figure 2A), in excellent agreement with Zaccolo et al. (*33*). Indeed, of 438 mutational events, 239 (54.6%) are represented by A → G transitions. The 54 (12.3%) T → C transitions result from the preferential incorporation of dPTP opposite A in either strand and subsequent pairing with G. The C → T and G →A transitions (due to incorporation of dPTP opposite G in either strand and subsequent pairing with A) constitute 18.3% and 14.8%, respectively.

To visualize the DNA curvature of the 11 pCf inserts, their sequences where subjected to computer analysis by our implementation of the CURVATURE prediction algorithm (*35*). Overall, the picture emerging from the in silico assays (Figure 2B) matches the PAGE pattern of Figure 1 quite strictly and confirms that the progressive decrease in *k* values observed by electrophoresis culminates with the complete removal of curvature in the insert of pCf19. The models suggest that in curved fragments the bend might not always be confined to a restricted region. It is also worth mentioning that the predicted shape of the wild-type fragment (pCf0 insert) shows a remarkable agreement with previously published EM images (*37*).

In essence, the mutation approach we have adopted has proven to be very effective in progressively "melting" the bent structure and generating a population of homogeneously sized fragments with progressively decreasing curvature, thus providing a spectrum of templates suitable for a systematic investigation of the effect of intrinsic bending on in vitro transcription.

Bending Analysis. We have addressed the issue of the general value of the relationship between intrinsic bending and efficiency of in vitro transcriptional activity by positioning the mutagenized fragments, obtained as described in the previous section, upstream from the promoter of a reporter gene. To this end, a specific vector, pCAT, has been constructed by cloning the *cat* gene from pACYC184, including its −10 and −35 boxes, into a pBR322 derivative just downstream from a unique BglII site located at position −42 from the *cat* transcription start site (Figure 3A). The 10 pCf inserts obtained upon in vitro mutagenesis, as well as the control insert from pCf0, were amplified by PCR, digested with BamHI and BglII, and cloned into the BglII site of pCAT. A BamHI restriction digestion of the pCATCf recombinants allowed us to easily identify those carrying the inserts in the same orientation. The wild-type *C. fasciculata* bent fragment is

known to form a small loop flanked by unbent arms, a short one and a longer one carrying a NruI site (*37*) (see also Figure 2A). The orientation selected for further studies was the one in which the shorter unbent arm was placed closer to the *cat* promoter, to position the bend at a distance (~140 nucleotides) from the *cat* transcription start compatible with that reported in genome-wide in silico surveys (*12*, *13*), which stress the presence of significant curvature among bacterial promoters −80 to −200 nucleotides upstream from the transcription start.

The inserts from the 11 pCATCf recombinants (pCATCf0, -2, -4, -5, -7, -8, -10, -11, -13, -14, and -19) were amplified by PCR. This gave rise to 271 bp fragments, containing the same 211 bp core as in the corresponding pCf inserts, flanked by short (30 bp) arms that encompass promoter regulatory elements up to and including the −10 box as well as a small region upstream from the BglII cloning site. The curvature of the 271 bp fragments was analyzed over the same temperature range (27.1−37.4 °C) used for the successive transcription assays. The data are reported as *k* values (ratio of the apparent size to the real size) in Figure 4A (top histogram series). With a decreasing temperature, a progressive curvature increase is apparent for all inserts except for the one from pCATCf19: its *k* value is the lowest ($k = 1.05$) over the entire temperature range analyzed and does not significantly increase even at 4 °C [$k = 1.08$ (not shown)], a clear indication that this insert is not bent. It is worth noting that at 4 °C the corresponding pCf insert [pCF19 (Figure 1)] has an identical curvature ($k = 1.07$), indicating that the two short arms flanking the 211 bp core in the pCATCf inserts are not curved, as confirmed also by computer predictions (not shown).

In Vitro Transcription. To verify the promoter promoting activity of DNA intrinsic curvature, we used the 11 pCATCf plamids mentioned above as templates in in vitro assays. The synthesis of nascent transcripts was monitored by a very sensitive real-time fluorescence-based approach (*34*). The setup we used allowed us to follow the transcriptional activity of all templates over the entire 27.1−37.4 °C temperature range in a single run. This was made possible by using an oligodeoxynucleotide molecular beacon (MB), constituted by short complementary ends framing a larger single-stranded stretch able to pair with an accessible region of the transcript. One end of the beacon is tagged with a fluorochrome (FAM), while the other is tagged with a fluorescence quencher (DABCYL). Under physiological conditions, the beacon forms a stem−loop structure keeping the fluorochrome and the quencher in the proximity of each other, so that no fluorescence can be emitted. Pairing of the beacon's loop to its complementary region on the nascent RNA target melts the stem and results in a measurable fluorescence signal due to the separation of the fluorochrome end from the quencher end.

The 24-nucleotide beacon we have used [*cat*-MB (Figure 3B)] forms a 5 bp double-stranded stem (5′-FAM-/3′-DABCYL-tagged) and a 14-nucleotide single-stranded loop. The 5′-portion of the stem and the entire loop are complementary to the *cat* gene region of nucleotides 448−462 which, by in silico analysis, appears to be able to form a stable single-stranded loop. We checked the specificity of the *cat*-MB probe by monitoring the fluorescence of agarose gel separations of individual pCATCf-driven reactions and of control reactions set up either with an unspecific template (pBR322), in the absence of RNAP, or in the absence of the *cat*-MB probe. None of the controls showed a *cat* mRNA band, while such a product became visible in the case of pCATCf-driven reactions (not shown). A further confirmation came from pairing the *cat*-MB probe with increasing

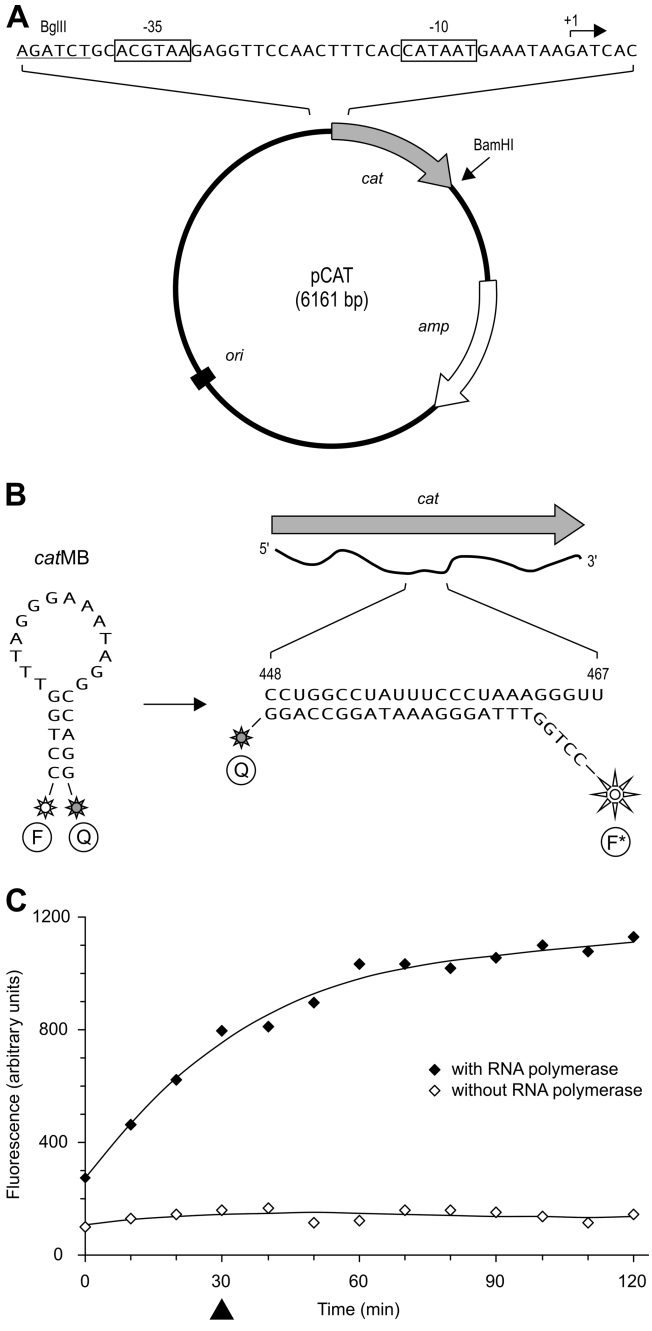

FIGURE 3: Setting up the in vitro transcription system. (A) Relevant features of the cloning vector (pCAT). pCAT contains a unique BglII site, which was used for cloning the Cf fragments. The *cat* reporter gene contains its natural promoter with the −10 and −35 box. (B) Structure and sequence of the *cat*-specific molecular beacon (*cat*-MB). In the absence of a specific target, the molecule forms a secondary structure (left) where the proximity of the quencher end (Q) to the fluorochrome end (F) prevents fluorescence emission. Pairing of the loop with the region of nucleotides 448−462 of the *cat* transcript (right) separates the two ends, thus activating the fluorochrome (F*). (C) In vitro transcription efficiency of the pCAT vector. The reaction between pCAT and *cat*-MB [10^{-4} mM (see Experimental Procedures)] was allowed to occur at a constant temperature in the presence or absence of *E. coli* RNAP, and progress was monitored in a fluorimeter (excitation wavelength of 485 nm, emission wavelength of 530 nm). The graph refers to a reaction run at 37.4 °C (each point is the average of at least three independent assays; the difference between the minimum and maximum observed values did not exceed 5.7% of the average). Analogous results (not shown) were obtained in assays conducted at lower temperatures (27.1, 28.5, 30.9, 33.6, and 36 °C), confirming the strict RNA polymerse dependency of the fluorescence emission. Reactions using the pCATCf templates (see the results in Figure 4) were allowed to proceed for 30 min (▲).

concentrations of specific anti-beacon DNA (a-*cat*-MB): fluorescence was found to be strictly proportional to the a-*cat*-MB concentration.

In a typical in vitro transcription assay, an array of six identical reaction mixtures was set up for each of the 11 pCATCf templates. Transcription was allowed to occur when all arrays were placed over a continuous temperature gradient. Within each array, the temperatures corresponding to positions 1−6 were 27.1, 28.5, 30.9, 33.6, 36, and 37.4 °C, respectively. Fluorescence intensity was monitored simultaneously on the whole array block, and final readings were taken after 30 min. Fluorescence emission was found to strictly depend on transcriptional activity and to be proportional to the amount of transcript, as confirmed by pCAT-driven control reactions (run under the same conditions and at the same temperatures used for the pCATCf templates) in the absence or presence of RNAP (Figure 3C).

The results are shown in Figure 4A (bottom histogram series) as 37 °C-normalized values. Comparing these data with the curvature values of the pCATCf inserts at the same temperatures (Figure 4A, top histogram series) indicates that, while in the template carrying an unbent insert (pCATCf19) the transcriptional activity exhibits a neat progressive reduction with a decrease in temperature, the response of templates carrying bent inserts is quite different: overall, in these templates transcription is significantly less sensitive to a temperature decrease. Moreover, template pCATCf5 shows the highest relative activity at the lowest temperature tested. In more curved templates (pCATCf4−pCATCf0), transcription peaks at progressively higher temperatures, and the same trend is also apparent (though to a somewhat lesser extent) for the less curved templates (pCATCf7−pCATCf19), thus pointing to the existence of a DNA curvature threshold that optimizes in vitro promoter activity. Averaging the transcription values within each temperature series [Figure 4A (○)] confirms that a quite specific level of DNA bending is required to maximize in vitro transcription. The overall trend of the average 37.4 °C-normalized transcription values is a biphasic one: with progressively increasing curvature promoter activity is first gradually, but significantly, enhanced (pCATCf19−pCATCf4, average k of 1.05−1.67 and average transcription of 0.77−1.16) and then quenched toward initial values (pCATCf2 and pCATCf0, average k values of 1.93 and 3.07 and average transcriptions of 0.96 and 0.84, respectively). Taking into account the fact that the templates originate from a random selection operated on a larger set (see figure 1), generated itself by random mutagenesis, it is quite unlikely that the observed trend might be ascribed mainly to the primary DNA sequence changes introduced by our mutagenesis procedure. Indeed, a search for UP elements [previously identified as possible enhancers of promoter activity (*39*)] in the pCATCf templates that have been analyzed does not reveal any significant homology.

At the evaluation stage shown in Figure 4A, the transcription data are affected not only by curvature but also by other variables, most notably RNAP activity, exhibiting temperature dependence. Hence, to factor out these variables and make the effect of DNA curvature alone stand out, we used the temperature-dependent in vitro transcription profile of the pCATCf19 template, which carries an unbent insert, as a relative temperature-by-temperature reference for the templates carrying curved inserts. The outcome of this normalization procedure is summarized in Figure 4B, where the transcriptional activity relative to the unbent control is shown as a contour plot in a temperature versus curvature graph. The data indicate that (a) with progressively

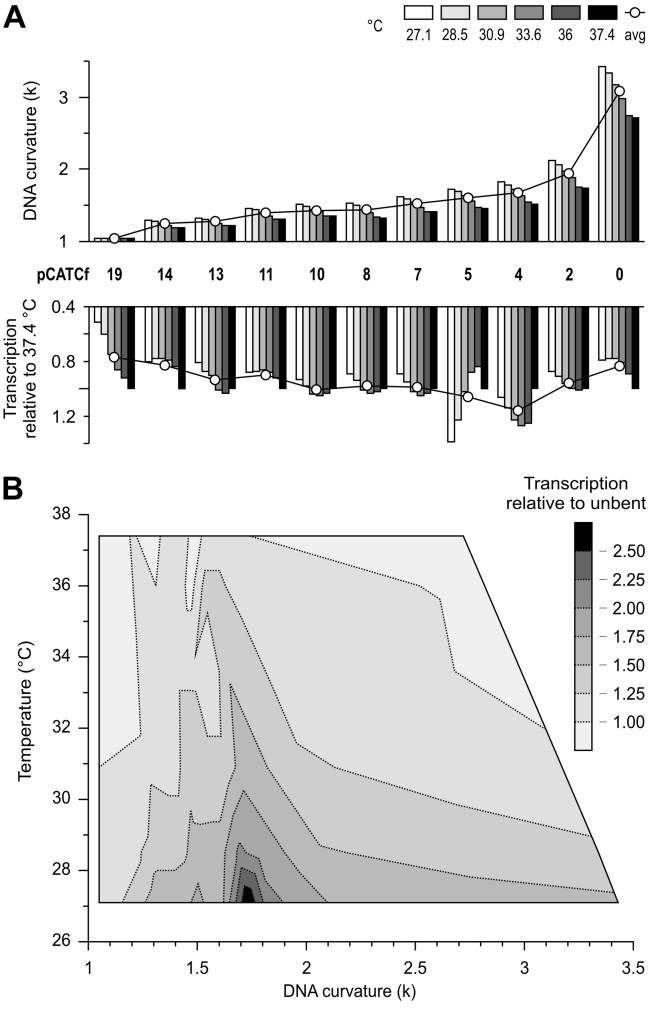

FIGURE 4: Temperature-dependent in vitro transcription of the pCATCf templates. (A) Comparison between the curvature of the 271 bp pCATCf inserts and the in vitro transcriptional activity of the corresponding plasmid templates. Both DNA curvature and in vitro transcription were assayed at 27.1, 28.5, 30.9, 33.6, 36, and 37.4 °C (empty circles indicate the average within a temperature series). Curvature was determined by polyacrylamide gel electrophoresis and is reported as a k value (ratio of the apparent size to the real size). In vitro transcription was allowed to proceed for 30 min (compare with Figure 3C). Template activity was monitored in real time using the *cat*-MB (Figure 3B), and results are shown as 37.4 °C-normalized values. Each curvature−transcription datum column represents the average of three to four independent experiments (the difference between the minimum and maximum observed values did not exceed 2.3% of the average in curvature assays or 6.1% of the average in transcription assays). (B) Temperature−curvature−transcription relationship. The temperature-dependent transcriptional profiles of the pCATCf templates carrying bent inserts [(A) pCATCf0, -2, -4, -5, -7, -8, -10, -11, -13, and -14] were normalized to the profile of the template carrying an unbent insert [pCATCf19 (A)]. The result is shown as a contour plot in a temperature vs DNA curvature (k) graph.

increasing DNA curvature transcription increases up to a maximum and then decreases and (b) this behavior becomes more and more evident with a decrease in temperature. This identifies a curvature interval that maximizes transcription: while at 36 °C the maximum (1.25-fold as compared to the unbent control) is reached at a k of 1.55, at 27.1 °C the peak (≥2.5-fold of the unbent control) is attained at a k of 1.73. Thus, in terms of transcriptional levels obtained under the conditions we have used, it is safe to assume that the reduction in RNAP activity induced by the decrease in temperature is more than compensated

by the increase in DNA curvature, and that this effect is particularly strong in a rather narrow curvature range.

Conclusions. Besides its static role, intrinsic DNA curvature offers further regulatory opportunities when exploited dynamically, i.e., in response to changing environmental conditions. The temperature dependence of sequence-mediated curvature exemplifies such a case. Efficient sensing of temperature variations may become a necessity for the quick adaptation of gene expression to rapidly changing environmental conditions. This is highly relevant to pathogenic microorganisms, which need to express virulence genes not in the outer environment but only when they have penetrated the warmer host milieu. Several strategies that fulfill this requirement have been described, involving changes both in RNA structure (*40*) and in protein structure (*41*), yet another mechanism relies on temperature-induced changes in the intrinsic curvature of gene promoters, making bent DNA act as a thermosensor (*18*−*21*, *23*). This strategy applies to several pathogenic bacteria and allows them to quickly match their transcriptional program to new environments. In bacterial promoters, an increased intrinsic DNA curvature not only appears to be able to favor the binding of activators (*9*, *10*, *23*) or repressors (*17*, *19*−*21*) but also has been reported to increase transcriptional activity per se, i.e., without the involvement of trans-acting regulators (*18*).

This prompted us to start investigating the as yet unanswered issue of the existence of a most favorable template curvature condition able to promote transcription in bacteria. By positioning fragments covering a large spectrum of DNA bending upstream from a promoter of a reporter gene and by studying its thermoregulated transcription, we have shown that, in a physiologically relevant temperature range, in vitro promoter activity is maximized over a quite narrow DNA curvature interval. The identification of such a threshold and the lack, in the templates tested, of UP sequence elements surmised to stimulate transcription (*37*) hint at the relevance of upstream template shape rather than stringent nucleotide sequence constraints. Overall, our observations, together with those from genome-wide studies (*12*−*16*, *22*) that evidence the widespread presence of bent sequences upstream from bacterial promoter sites, support the view that DNA curvature-mediated regulation of gene expression is likely a regulatory strategy offering fine-tuning control possibilities and may represent one of the most primitive forms of gene regulation before the co-evolution of trans-acting factors able to recognize the bending level of the promoters.

ACKNOWLEDGMENT

We thank Prof. Ernesto Di Mauro for critical reading of the manuscript.

REFERENCES

1. Lukeš, J., Hashimi, H., and Zíková, A. (2005) Unexplained complexity of the mitochondrial genome and transcriptome in kinetoplastid flagellates. *Curr. Genet. 48*, 277–299.
2. Haran, T. E., and Mohanty, U. (2009) The unique structure of A-tracts and intrinsic DNA bending. *Q. Rev. Biophys. 42*, 41–81.
3. Crothers, D. M., Haran, T. E., and Nadeau, J. G. (1990) Intrinsically bent DNA. *J. Biol. Chem. 265*, 7093–7096.
4. Diekmann, S., and Wang, J. C. (1985) On the sequence determinants and flexibility of the kinetoplast DNA fragment with abnormal gel electrophoretic mobilities. *J. Mol. Biol. 186*, 1–11.
5. Travers, A. A. (1989) DNA conformation and protein binding. *Annu. Rev. Biochem. 58*, 427–452.
6. Travers, A. A. (1995) DNA bending by sequence and protein. In DNA-Protein Structural Interactions (Lilley, D. M. J., Ed.) pp 49−75, Oxford University Press, New York.
7. Garcia, H. G., Grayson, P., Han, L., Inamdar, M., Kondev, J., Nelson, P. C., Phillips, R., Widom, J., and Wiggins, P. A. (2007) Biological consequences of tightly bent DNA: The other life of a macromolecular celebrity. *Biopolymers 85*, 115–130.
8. Ohyama, T. (2001) Intrinsic DNA bends: An organizer of local chromatin structure for transcription. *BioEssays 23*, 708–715.
9. Pérez-Martín, J., Rojo, F., and de Lorenzo, V. (1994) Promoters responsive to DNA bending: A common theme in prokaryotic gene expression. *Microbiol. Rev. 58*, 268–290.
10. Perez-Martin, J., and de Lorenzo, V. (1997) Clues and consequences of bending in transcription. *Annu. Rev. Microbiol. 51*, 593–628.
11. Jáuregui, R., O'Reilly, F., Bolivar, F., and Merino, E. (1998) Relationship between codon usage and sequence-dependent curvature of genomes. *Microb. Comp. Genomics 3*, 243–253.
12. Gabrielian, A. E., Landsman, D., and Bolshoy, A. (1999) Curved DNA in promoter sequences. *In Silico Biol. 1*, 183–196.
13. Bolshoy, A., and Nevo, E. (2000) Ecologic genomics of DNA: Upstream bending in prokaryotic promoters. *Genome Res. 10*, 1185–1193.
14. Kozobay-Avraham, L., Hosid, S., and Bolshoy, A. (2004) Curvature distribution in prokaryotic genomes. *In Silico Biol. 4*, 361–375.
15. Kozobay-Avraham, L., Hosid, S., and Bolshoy, A. (2006) Involvement of DNA curvature in intergenic regions of prokaryotes. *Nucleic Acids Res. 5*, 2316–2327.
16. Jáuregui, R., Abreu-Goodger, C., Moreno-Hagelsieb, G., Collado-Vides, J., and Merino, E. (2003) Conservation of DNA curvature signals in regulatory regions of prokaryotic genes. *Nucleic Acids Res. 31*, 6770–6777.
17. Prosseda, G., Falconi, M., Giangrossi, M., Gualerzi, C. O., Micheli, G., and Colonna, B. (2004) The *virF* promoter in *Shigella*: More than just a curved DNA stretch. *Mol. Microbiol. 51*, 523–537.
18. Katayama, S., Matsushita, O., Jung, C., Minami, J., and Okabe, A. (1999) Promoter upstream bent DNA activates the transcription of the *Clostridium perfrigens* phospholipase C gene in a low temperature-dependent manner. *EMBO J. 18*, 3442–3450.
19. Falconi, M., Colonna, B., Prosseda, G., Micheli, G., and Gualerzi, C. O. (1998) Thermoregulation of *Shigella* and *Escherichia coli* EIEC pathogenicity. A temperature-dependent structural transition of DNA modulates accessibility of *virF* promoter to transcriptional repressor H-NS. *EMBO J. 17*, 7033–7043.
20. Rohde, J. R., Luan, X. S., Rohde, H., Fox, J. M., and Minnich, S. A. (1999) The *Yersinia enterocolitica* pYV virulence plasmid contains multiple intrinsic DNA bends which melt at 37 °C. *J. Bacteriol. 181*, 4198–4204.
21. Madrid, C., Nieto, J. M., Paytubi, S., Falconi, M., Gualerzi, C. O., and Juárez, A. (2002) Temperature- and H-NS-dependent regulation of a plasmid-encoded virulence operon expressing *Escherichia coli* hemolysin. *J. Bacteriol. 184*, 5058–5066.
22. Olivares-Zavaleta, N., Jáuregui, R., and Merino, E. (2006) Genome analysis of *Escherichia coli* promoter sequences evidences that DNA static curvature plays a more important role in gene transcription than has previously been anticipated. *Genomics 87*, 329–337.
23. Giladi, H., Goldenberg, D., Koby, S., and Oppenheim, A. (1995) Enhanced activity of the bacteriophage λ PL promoter at low temperature. *Proc. Natl. Acad. Sci. U.S.A. 92*, 2184–2188.
24. Dorman, C. J., and Deighan, P. (2003) Regulation of gene expression by histone-like proteins in bacteria. *Curr. Opin. Genet. Dev. 13*, 179–184.
25. Prosseda, G., Falconi, M., Nicoletti, M., Casalino, M., Micheli, G., and Colonna, B. (2002) Histone-like proteins and the *Shigella* invasivity regulon. *Res. Microbiol. 153*, 461–468.
26. Falconi, M., Prosseda, G., Giangrossi, M., Beghetto, E., and Colonna, B. (2001) Involvement of FIS in the H-NS-mediated regulation of *virF* gene of *Shigella* and enteroinvasive *Escherichia coli*. *Mol. Microbiol. 42*, 439–452.
27. Luijsterburg, M. S., Noom, M. C., Write, G. J., and Dame, R. T. (2006) The architectural role of nucleoid-associated proteins in the organization of bacterial chromatin. A molecular perspective. *J. Struct. Biol. 156*, 262–272.
28. Travers, A., and Muskhelishvili, G. (2005) Bacterial chromatin. *Curr. Opin. Genet. Dev. 15*, 507–514.
29. Dorman, C. J. (2004) H-NS: A universal regulator for a dynamic genome. *Nat. Rev. Microbiol. 2*, 391–400.
30. Fang, F. C., and Rimsky, S. (2008) New insights into transcriptional regulation by H-NS. *Curr. Opin. Microbiol. 11*, 113–120.
31. Sambrook, J., and Russell, D. (2001) Molecular cloning: A laboratory manual, 3rd ed., Cold Spring Harbor Laboratory Press, Plainview, NY.
32. Kitchin, P. A., Klein, V. A., Ryan, K. A., Gann, K. L., Rauch, C. A., Kang, D. S., Wells, R. D., and Englund, P. T. (1986) A highly bent

fragment of *Crithidia fasciculata* kinetoplast DNA. *J. Biol. Chem. 25*, 11302–11309.
33. Zaccolo, M., Williams, D. M., Brown, D. M., and Gherardi, E. (1996) An approach to random mutagenesis of DNA using mixtures of triphosphate derivatives of nucleoside analogues. *J. Mol. Biol. 255*, 589–603.
34. Liu, J., Feldman, P., and Chung, T. D. (2002) Real-time monitoring *in vitro* transcription using molecular beacons. *Anal. Biochem. 300*, 40–45.
35. Shpigelman, E. S., Trifonov, E. N., and Bolshoy, A. (1993) CURVATURE: Software for the analysis of curved DNA. *COBIAS, Comput. Appl. Biosci. 9*, 435–440.
36. Matzura, O., and Wenneborg, A. (1996) RNAdraw: An integrated program for RNA secondary structure calculation and analysis under 32-bit Microsoft Windows. *COBIAS, Comput. Appl. Biosci. 12*, 247–249.
37. Griffith, J., Bleyman, M., Rauch, C. A., Kitchin, P. A., and Englund, P. T. (1986) Visualization of the bent helix in kinetoplast DNA by electron microscopy. *Cell 46*, 717–724.
38. Diekmann, S. (1987) Temperature and salt dependence of the gel migration anomaly of curved DNA fragments. *Nucleic Acids Res. 15*, 247–265.
39. Estrem, S. T., Ross, W., Gaal, T., Chen, Z. W., Niu, W., Ebright R. H., and Gourse, R. L. (1999) Bacterial promoter architecture: Subsite structure of UP elements and interactions with the carboxy-terminal domain of the RNA polymerase α subunit. *Genes Dev. 13*, 2134–2147.
40. Johansson, J., Mandin, P., Renzoni, A., Chiaruttini, C., Springer, M., and Cossart, P. (2002) An RNA thermosensor controls expression of virulence genes in *Listeria monocytogenes*. *Cell 110*, 551–561.
41. Ono, S., Goldberg, M. D., Olsson, T., Esposito, D., Hinton, J. C., and Ladbury, J. E. (2005) H-NS is a part of a thermally controlled mechanism for bacterial gene regulation. *Biochem. J. 391*, 203–213.